CGU HS Committee on River Ice Processes and the Environment
16th Workshop on River Ice
Winnipeg, Manitoba, September 18 – 22, 2011

Hydraulic experiment on river ice floes transport due to bore tsunami run-up

Takaaki ABE[1], Yasuhiro YOSHIKAWA[1], Hiroyasu YASUDA[2], Yasuyuki HIRAI[1]

[1]*Civil Engineering Research Institute for Cold Region, River Engineering Research Team*
Hiragishi 1-3, Toyohira-ku, Sapporo 062-7602 Japan
abe-t@ceri.go.jp

[2]*Niigata University Research Institute for Natural Hazards & Disaster Recovery*
8050, Ikarashi 2-Nocho, Nishi-ku, Niigata 950-2181 Japan
hiro@gs.niigata-u.ac.jp

In this study, the authors performed a series of laboratory experiments to examine the drift motion of ice floes driven by bore-like tsunamis. The work involved investigating the disintegration of a tsunami into a train of undular bores with floating ice models on the surface. The experiments were recorded using digital cameras, and ice floe positions were determined as a function of time from digitalized pictures using the PTV image analysis technique. A number of interesting findings were made from these experiments. It was observed that the run-up heights of wave fronts increased by over 70% in the wave propagation process, and that the time-series waveforms of undular bores closely corresponded to model tracer velocities. This means that bore fronts are capable of causing sudden large acceleration in the movement of ice floes. The outcomes highlighted the potential risks of these masses of ice, which can be hazardous to river structures such as bridge piers, floodgates and intake screens.
Keywords: undular bore, tsunami run-up, frozen rivers, ice floe transportation

1. Introduction

1.1 Study Background

Large earthquakes with a magnitude of 8.0 or greater and subsequent massive tsunamis exceeding 10 m in height occur along the Japan Trench and the Kuril Trench. Major tremors have also frequently hit the Hokkaido region off the coast of Kushiro, southwest Hokkaido, Tokachi and other areas in the last 20 years. On March 11, 2011, a devastating earthquake hit the area off the Sanriku Coast (an event that had been increasingly feared and whose imminent risk had been pointed out by many experts), causing massive loss of life and damage to property in Miyagi, Iwate and the surrounding areas. Efforts have long been made to develop master plans and prioritize facility improvements in order to protect the lives and property of people in Japan from earthquakes and other disasters. However, in the wake of the extensive damage caused by this massive earthquake and tsunami, a fundamental review of safety standards for disaster prevention facilities and disaster protection countermeasures is called for. Cold snowy regions such as Hokkaido are especially required to prepare for complex disasters that may occur in winter on the assumption that a tsunami caused by a major earthquake will reach inland areas.

In the 2004 earthquake in the Indian Ocean off Sumatra, tsunamis running up rivers and causing enormous damage to bridges and other structures were reported in many countries. This led to a keen realization of the dangers of tsunami run-up. In the front part of a tsunami traveling up a shallow water channel such as a river, undular bores accompanied by a rise in the local water level are formed. A recent study[2)] revealed that there were significant rises in water level – by factors of approximately 1.4 in still water and from approximately 2.0 - 2.5[3)] in flowing water – compared to the incident wave height. The Indian Ocean Tsunami swallowed up coastal houses, vessels, timber, vehicles and other property, and the resulting flow of debris further destroyed and crushed other structures, in turn producing large amounts of flotsam and exacerbating the damage[4)]. A massive earthquake in the Hokkaido area in winter may cause tsunamis to enter and run up frozen rivers and transport river ice floes, which are likely to damage river structures.

Photo 1 shows an ice floe near point KP 0.8 on the left bank of the Mu River (Pacific coast, Hokkaido). This mass of ice is considered to have been transported by a tsunami caused by the 2011 Tohoku Pacific Coast Earthquake. Although the floe had cracks in its middle part, it measured approximately 7 m long, 3 m wide and 25 cm thick, and weighed an estimated 4.7 tons assuming a specific gravity of 0.9. Tsunami-induced changes in water level at the Mu River Gauging Station (KP 2.55) were reported to be up to approximately 80 cm[5)]. However, huge ice floes similar to the one shown in the photo were found in various places from the estuary to areas where the tsunami arrived. A major earthquake in the seas around Hokkaido can be expected to generate a tsunami that would penetrate further inland with an even greater level of energy. In a previous case, a tsunami caused by the 1952 Tokachi-Oki earthquake swept up the Harutori River in Kushiro City, breaking up river ice and causing ice floes to flow over levees and damage houses[6)].

Damage scenarios assuming the transportation of floating ice floes by a tsunami running up a river are as follows

I. The wave breaks ice floes into pieces, which block sluices/floodgates and obstruct their operations
II. Ice floes travel upstream and crash into bridges and other cross-river structures, causing damage to bridge piers and displacement of supports as well as collateral damage to railways and vehicles on bridges.

The various measures that can be promoted to protect boats moored on rivers and lumber stored in yards from disasters include implementing enhanced boat mooring practices, enforcing relevant regulations and improving related systems. However, the annual formation of ice floes in rivers is a natural phenomenon characterized by constant variations in thickness, location and length depending on meteorological conditions. Ice floes differ from other floating objects in that they are fragile and rupture easily upon impact with structures. Accordingly, there is a need for region-specific disaster protection measures that take these characteristics into account.

Against this background, the formulation of tsunami countermeasures requires an assessment tool that allows estimation of the distance and velocity with which ice floes will transported up a river by a tsunami. However, it is currently not possible to assess the safety of river structures based on clearly defined criteria because there have been very few studies on the behavior of floating objects transported by tsunamis running up rivers, and there is also a lack of recorded data on damage caused by such conditions.

1.2 Past Studies

There have been numerous studies on floating objects transported by tsunamis in coastal areas. Ikeno et al.[7) – 8)] summarized the relationship between the force of tsunami waves that transport floating objects and affect structures while running up rivers and the movement and collision force of such objects in various shapes. To investigate floating objects affected by tsunamis, Mizutani et al.[9)] examined containers on an apron, and Iketani[10)] et al. investigated anchored boats to enable the proposal of a method for assessing the collision force of such objects. Although a limited number of studies[11) – 12)] have also examined the transportation of sea ice floes by tsunamis, it is difficult to immediately apply the findings of these investigations because they focused on the movement of a single floating object[8)] or did not consider the effects of dispersive wave train influences such as undular bores[12)].

As described in the previous section, the distance of ice floe run-up (which could serve as an index to predict the related influence on river structures in affected areas) and its velocity (which affects tsunami wave force) were considered in the development of tsunami disaster protection plans for rivers. In this regard, there is a need to establish a practical method for identifying areas at risk.

Accordingly, hydraulic experiments on river ice floes were performed in this study with the aim of clarifying the characteristics of ice floe transportation by undular bores – something that has not been closely examined in past studies. The experiments simulated thin ice floes floating on a river. The goals were to clarify the nature of interaction between tsunami run-up and ice floes, and to elucidate the effects of water depth at the initial position of ice floes and tsunami wave height on the process of ice floe transportation.

2. Overview of Tsunami Run-up Experiments Involving Ice Floes

2.1 Experimental Flume

A flume measuring 34 m in length and 0.5 m in width with a rectangular cross section (Fig. 1) was used in the hydraulic experiments. Artificial turf was laid over a steel girder on the flume bottom as shown in the figure. The area within 6 m of the downstream end was within the movement range of the wave paddle used, and the slope in this area was fixed. The flume slope was adjustable over a distance of 28 m from this area. A water supply mechanism at the upstream end and a drainage mechanism at the downstream end were installed as a combination capable of creating non-uniform flow fields. A buffer was placed at the upstream end to prevent the flowing water from being disturbed by the water supply. To measure changes in water level, capacitance-type wave gauges (made by KENEK Corporation, Japan) were installed at x = 5.0, 10.0, 15.0, 17.5 and 20.0 m (referred to as Ch. 1 through 5 in this paper) in the longitudinal direction.

Two digital cameras were installed above the experimental flume to record the process of ice floe transportation by a tsunami. Pass points were set on the top of the flume with the downstream end set as the origin (x = 0.0 m) at 1 m intervals from 0.5 m in the shooting range to facilitate clarification of the relative positions of tsunami waves and ice floes from video images.

2.2 Experimental Conditions

The limitations of the experimental facility made it difficult to reproduce a tsunami running up a river using a distortionless model. For this reason, a bed slope value of i = 1/250 and a water depth in front of the wave paddle equivalent to D_M = 0.80 m were used in all the experiments in line with the concept of distortion models in order to satisfy the requirement for Froude number similarity. The inflow discharge values were set to Q_{in} = 2.5, 5.0 and 7.5 [l/s] for the sake of convenience. These conditions represented the situation in a river section of approximately 5 km in the longitudinal direction with a water depth of approximately 4 m near the estuary, with observations made over a 25 m section of the experimental flume. The experimental discharge rates, which corresponded to values of approximately 80 – 110 m^3/s on site, were based on discharge figures recorded from the Class A Tokachi River (Hokkaido, Japan) between February and March (freezing – thawing seasons).

2.3 Ice Floe Model

A variety of ice floes are found in rivers; they may be broken pieces from completely frozen ice masses, ice strips attached to river banks, or ice floes accumulated in certain areas due to the effects of bridge piers and other objects. For simplification, accumulated ice floes were examined in this study because 1) they are easily transported by incident tsunamis, and 2) interaction between ice floes and riverbanks was considered negligible. Specifically, the target of investigation was a group of ice floes that had accumulated densely in a certain area (Photo 2) and were in the early stages of being carried up the river by a tsunami. To reproduce this event, polypropylene sheets measuring 30 mm in length, 30 mm in width and 5 ± 0.5 mm in thickness with a specific gravity of approximately 0.9 were used as ice floe models.

As it was difficult to reproduce multiple ice floes fixed in certain positions as shown in Photo 2 under experimental conditions with water flowing in, the number of ice floes used in

these experiments was limited to four. A tension rod was inserted along the bed, then two pieces of wire were tied to the rod for each ice floe and pulled upward to fix the floe positions vertically. This was intended to simulate accumulated ice floes in the uppermost part of the stream. However, it was difficult to evaluate the extent to which the presence of the bed-mounted tension rod and the wire affected the flow. This process will be considered further to determine a method for fixing ice floes in a flume while minimizing the related effects on tsunami propagation. The PTV image analysis technique, which is explained below, extracts tracer particles based on color differences. To facilitate individual identification of the four ice floe models' movement, they were colored blue, pink, yellow and light green (from left to right).

Under the conditions described above, an experiment was conducted by setting the group of ice floe models at the initial position (hereinafter referred to as D_{up}) in alignment with one of the wave gauges over a length stretching from approximately x = 5.0 m to 20.0 m in the flume and then changing the initial position for subsequent experiments.

3. Experimental Results

3.1 Wave Gauge Measurements

First, the extent to which the presence of ice floes affected tsunami behavior was examined. In a previous paper[13], the authors reported on an experiment involving a number of ice floes in static water and demonstrated that their presence had only a small effect on the deformation process and tsunami propagation velocity. For the two cases where the ice floes were positioned immediately upstream of the wave gauge (D_{up} = 5.0 before the formation of a dispersive wave train; D_{up} = 17.5 immediately before the breaking of the leading wave crest in the presence of water flows), time-series waveforms obtained by the wave gauges for three different water supply rates are shown in Figs. 3 (a) – (c). In these figures, t = 0.0 sec indicates the time at which the wave paddle was activated. Waveforms after t = 25.0 sec are not shown, as this was the point at which Ch. 5 began to be affected by reflected waves from the upstream end of the flume.

When a convex half-sine solitary wave (tsunami) was generated by the wave paddle, the tsunami deformed in the process of running up the flume in a similar way for all discharge rates. In addition, there was little difference in the deformation process associated with run-up between the ice floes located downstream at D_{up} = 5.0 and those located at D_{up} = 17.5.

In regard to the wave deformation process, the waveform that was initially almost symmetrical to the wave crest was transformed during propagation, and the leading wave took on a bore-like shape. At Ch. 3 (x = 15.0), a dispersive wave train with three to four wave crests was formed at the head in all cases. The first crest continued to develop until Ch. 4. For Q_{in} = 7.5, the maximum wave height increased from 6.4 cm initially to approximately 11 cm. This means the water level increased by as much as 70%, thereby exceeding the maximum wave height of 9 cm[13] (a water level increase of approximately 40%) observed in the previous experiment conducted in still water. As studies on the rise in tsunami run-up height in flow fields are still in their early stages[14], further research needs to be carried out to elucidate the related hydrodynamic characteristics.

At Ch. 5, the peak water level was seen to shift to the second or third wave crest in all cases. This was caused by wave breaking, in which the rapidly developed leading wave crest of a dispersive wave train collapsed because it could no longer support its own weight. Video images confirmed that the broken wave crests had small concave and convex surfaces. In general, it is considered that thin ice floes with the size of those used in the experiments minimally affect time-series tsunami waveforms, regardless of their location in the flume in the longitudinal direction. In other words, it is understood that the presence of groups of ice floes has little effect on tsunami wave height and wave crest travel velocity.

3.2 Discussion of Ice Floe Transportation Velocity in Relation to PTV Analysis

Ice floe transportation velocity ($\boldsymbol{U}_i$ m/sec) was determined from PTV analysis of ice floe transportation filmed and recorded as continuous images with two cameras. Dipp-Flow version 2.00 (DITECT Co., Ltd., Japan) was used for image analysis, and lens distortion correction/time-space correction were performed. In the experiments, four models were simultaneously transported by a tsunami, and their velocity values, which could be determined from tracer particles, were plotted over time. The ice floe models were mainly transported smoothly on the water surface of the tsunami run-up. However, when ice floe transportation involved breaking of the leading wave crest, some floes were pulled below the water surface and could not be detected as tracer particles.

Figures 4 and 5 show time-series variations of ice floe velocity components in the longitudinal direction for water supply rates Q_{in}= 2.5 *l*/s and 5.0 *l*/s. Here, velocities in the direction from the downstream to the upstream part of the flume are expressed as positive values. For comparison, changes in wave height for each case are shown at the top of the figures. It can be considered that the ice floe velocity waveforms for each value of D_{up} presented in the second through the sixth figures are related to incident waves that have waveforms as shown in the top figure.

In the case of D_{up} = 5.0 in Fig. 4, as the incident wave had a waveform with a single peak, the ice floe transportation velocity waveform also had a single peak. For D_{up} = 10.0, the transportation velocity waveform responded to a slightly steep slope in the water surface at the front of the incident wave and followed its shape. At D_{up} = 15.0, when the leading wave began to form a dispersive wave train, the transportation velocity waveform also showed a train of waves. At D_{up} = 10.0, the maximum transportation velocity, which had been approximately 0.5 m/s, rapidly increased to approximately 0.7 m/s. The development of the dispersive wave train continued until D_{up} = 17.5, and the ice floe transportation velocity waveform also became steep with a maximum value of 1.2 m/s – more than double that for D_{up} = 5.0 recorded before the formation of the dispersive wave train. An incident wave seen after wave breaking created a disturbance on the water surface, causing the ice floe models to sink and making it difficult to identify tracer particles in PTV analysis. As a result, the number of plot points decreased.

Figure 5 shows time-series waveforms for Q_{in} = 5.0 (top) and ice floe transportation velocity waveforms. These figures also confirm that transportation velocity waveforms varying with ice floe location were very similar to the waveforms seen in the tsunami deformation process. A similar trend was also found for Q_{in} = 7.5, although the details are omitted here due to space limitations.

Numerical simulation was conducted using one-dimensional unsteady flow calculation[15] to further examine the relationship between the waveform of a train of dispersive waves running up the flume and the ice floe transportation process. As an example, temporal changes in ice floe transportation velocity U_{ice} are shown in Fig. 6 (a), and calculated values of depth averaged velocity U_{ave} and water levels at ice floe locations are shown in Fig. 6 (b) and Fig. 6 (c), respectively, for conditions of Q_{in} = 5.0 and D_{up} = 17.5. The ice floe locations found from image analysis were based on discrete values. Among these locations, four points corresponding to dispersive wave train crests, three points at wave bottoms and two points from after the disappearance of short-periodic changes in the water level of the dispersive wave train were extracted and plotted. Comparison of Figs. 6 (a), (b) and (c) shows that U_{ice} reached its maximum value almost at the same time as the wave crest passed under the ice floes. When the floes fell to the wave bottom, both U_{ice} and U_{ave} were found to be at their lowest. Subsequently, when the second wave crest passed the point where the ice floes were located, U_{ice} again had a large value. After approximately t = 19.0 sec when the effect of the dispersive wave train's amplitude disappeared, U_{ice} decreased monotonically.

Based on the above, it is known that the velocity of ice floes is increased by the steep water surface slope of the leading wave crest of a tsunami or by the second wave crest of the dispersive wave train, and that it is rapidly reduced when the floes are at the bottom of the dispersive wave train. In the early stages of the transportation process, such intermittent acceleration and deceleration are repeated. After the disappearance of water level changes caused by the tsunami and the subsequent dispersive wave train, both of which transport ice floes, the floes are assumed to be transported solely by the effects of surface movement.

3.3 Discussion on Wave Height-Water Depth Ratio and Maximum Ice Floe Transportation Velocity

In this section, the relationship between the ratio of incident wave-height to water depth and the ratio of the maximum ice floe transportation velocity to the tsunami propagation velocity is examined using the results of the experiments along with those from an experiment conducted in a previous study[13] using a discharge of Q_{in} = 0.0 in order to clarify how fast ice floes would run upstream under the effects of increased wave height. An index to indicate the scale of a tsunami was created by dividing the tsunami wave height η by the water depth at the initial ice floe position H_{ice}. The wave gauge installation positions in the experiment at Q_{in} = 0.0 from the previous report were the same as those in this study. For this reason, it was not possible to evaluate incident wave height for ice floes positioned between wave gauges. The tsunami wave height at points without a wave gauge was calculated via numerical simulation as outlined in the previous section. As a number of ice floe models were used in the experiment in a zero discharge condition, different transportation characteristics were expected. However, the behavior of ice floes positioned in the uppermost part of the stream can be considered similar to that seen here provided that the ice floe models are regarded as accumulated floes as with the simulation in this study.

In the experiment with Q_{in} = 0, D_{up} was set with 1 m intervals, and in the experiment with water flows, it was set at the wave gauge installation locations. The maximum ice floe transportation velocity values obtained from PTV analysis were divided by the propagation

velocity of the first wave crest C_P and plotted for each experiment, and are given in Fig. 7. It was found that the maximum value for U_{ice} in each case increased monotonically with higher values of η/H_{ice}. In the region where η/H_{ice} < approx. 0.55, the increase was mild, whereas in other regions, the maximum value of U_{ice} increased sharply. As this trend was applicable to all cases regardless of the discharge rate, it can be concluded that ice floe transportation velocity is strongly affected by the wave height-water depth ratio.

The increase in values for incident waves after the formation of a dispersive wave train stagnated as (the maximum value of U_{ice})/C_P approached 1. This is assumed to be a result of the propagation velocity of the tsunami itself reaching the upper limit of the ice floe transportation velocity.

4. Summary

In this study, tsunami run-up experiments were carried out using ice floe models positioned on the water surface to simulate accumulated floes, wave height analysis was performed using wave gauges, and image analysis was conducted using recorded video images with the objective of examining the characteristics of ice floe transportation in relation to a tsunami running up a river and forming undular bores. The findings are summarized below.

・It was clarified that the presence of small thin ice floes would have only a small effect on the velocity of a tsunami. Under such conditions, time-series waveforms of ice floe transportation velocity were found to vary in a similar way to tsunami waveforms.
・For undular bores running up frozen rivers in winter, it was found that the maximum wave height could increase by a factor of approximately 1.7 due to discharge from the upstream area, and if ice floe transportation was involved, the velocity of ice floe run-up also increased sharply. It was thus clarified that there is a need to consider the effects of tsunami wave dispersion when evaluating the impacts of floating ice floes on structures in the event of a tsunami.
・It was seen that ice floe transportation velocity increases to the same level as the propagation velocity of the tsunami itself if the wave height-water depth ratio is high.

These experiments were performed to provide basic information on tsunamis and ice floe transportation; no in-depth study has yet been conducted to examine the extent to which wall friction and the presence of wave gauges affect flow fields and the process of ice floe spread. Continuous efforts are needed to identify appropriate settings for experimental conditions. Further studies are also needed to examine changes in the relationship between the process of ice floe transportation and ice floes themselves if they are thicker or larger than those used in this study.

Photo 1. Giant ice floe left in the flood channel of the Mu River at its estuary (March 14, 2011).

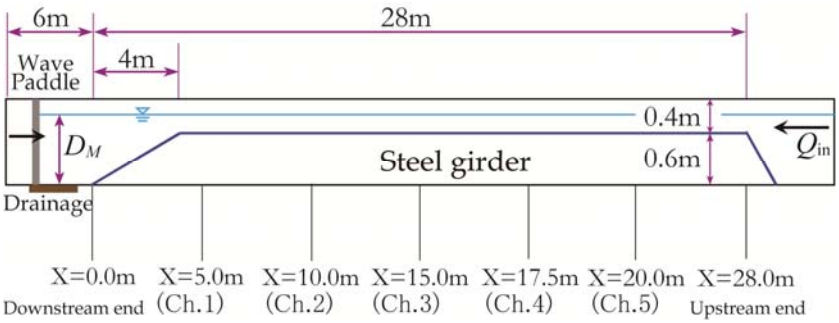

Figure 1. Experimental flume dimensions and wave gauge installation points (side view).

Photo 2. Numerous ice floes accumulated at bridge piers in an actual river (February 2009).

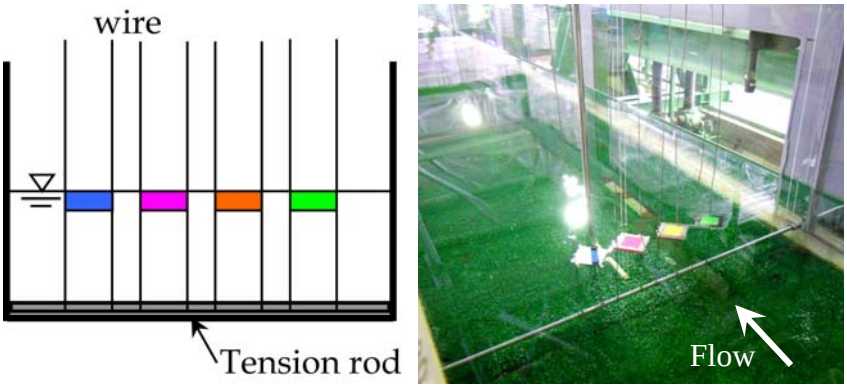

Figure 2. Scheme of ice floe models (cross section) and photo of installed models.

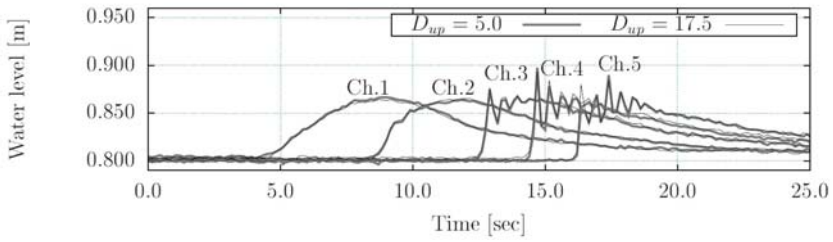

(a) Water level changes at each wave gauge (Q_{in} = 2.5 [l/s])

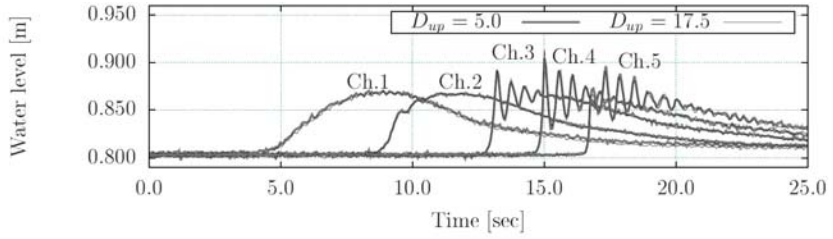

(b) Water level chan,es at each wave gauge (Q_{in} = 5.0 [l/s])

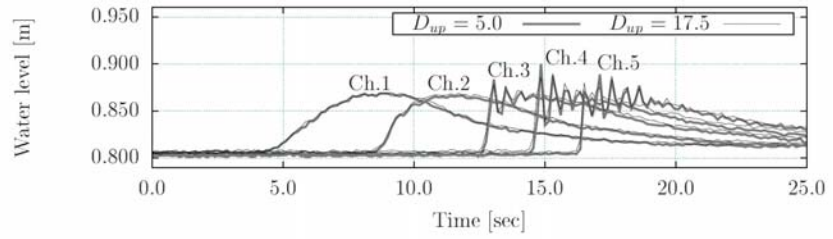

(c) Water level changes at each wave gauge (Q_{in} = 7.5 [l/s]).

Figure 3. Time-series waveforms obtained from hydraulic experiments (i = 1/250, D_M = 0.80, D_{up} = 5.0, 17.5).

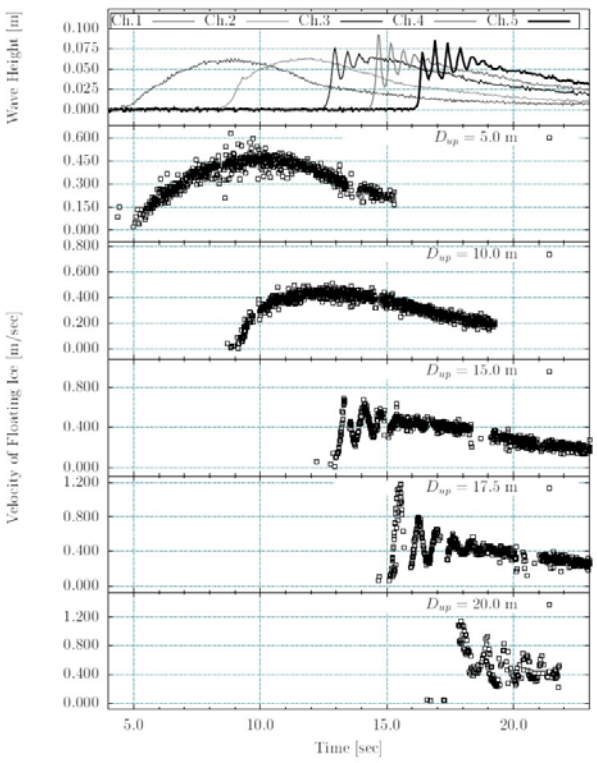

Figure 4. Temporal changes in tsunami wave height and ice floe transportation velocity based on wave gauge measurements (Q_{in} = 2.5).

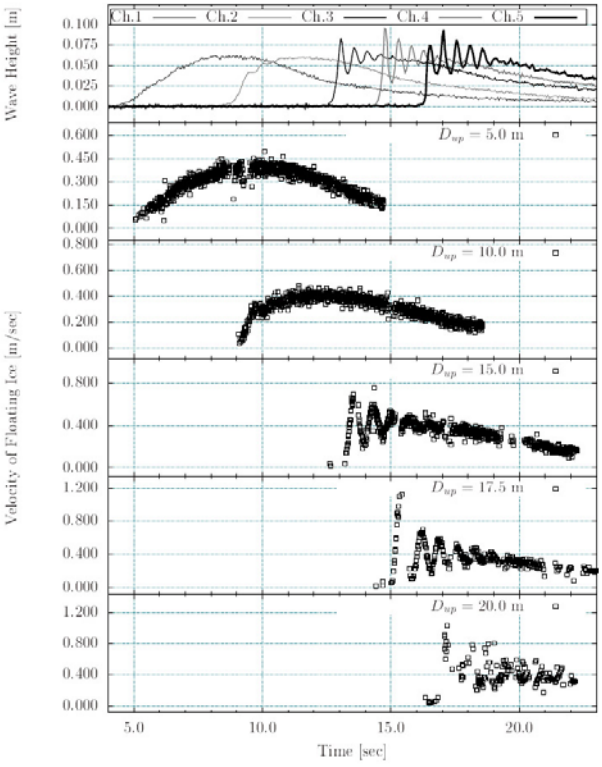

Figure 5. Temporal changes in tsunami wave height and ice floe transportation velocity based on wave gauge measurements (Q_{in} = 5.0).

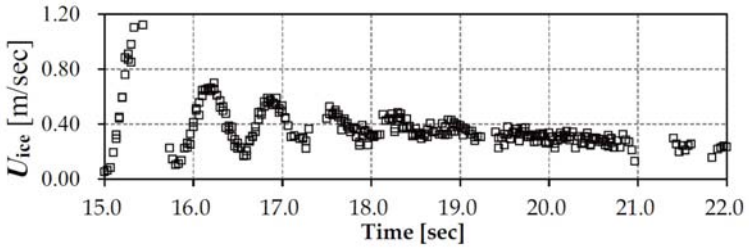

(a) Temporal changes in ice floe velocity.

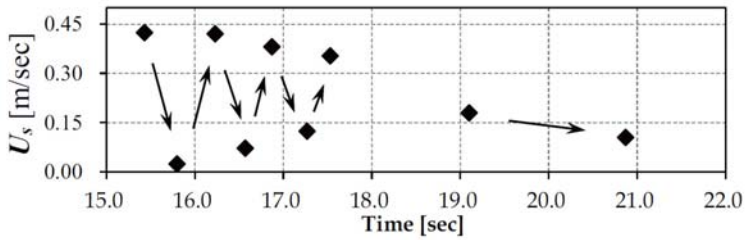

(b) Temporal changes in depth averaged velocity at ice floe locations.

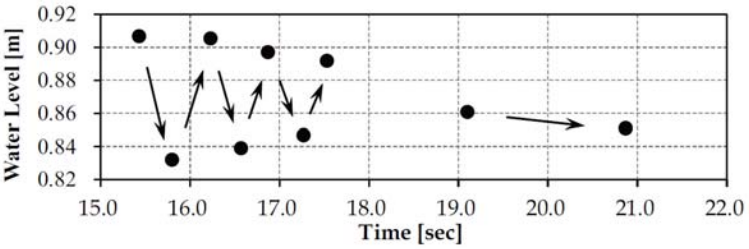

(c) Temporal changes in water levels at ice floe locations.

Figure 6. Temporal changes in ice floe velocity, depth averaged velocity and water levels at ice floe locations (Q_{in} = 5.0, D_{up} = 17.5).

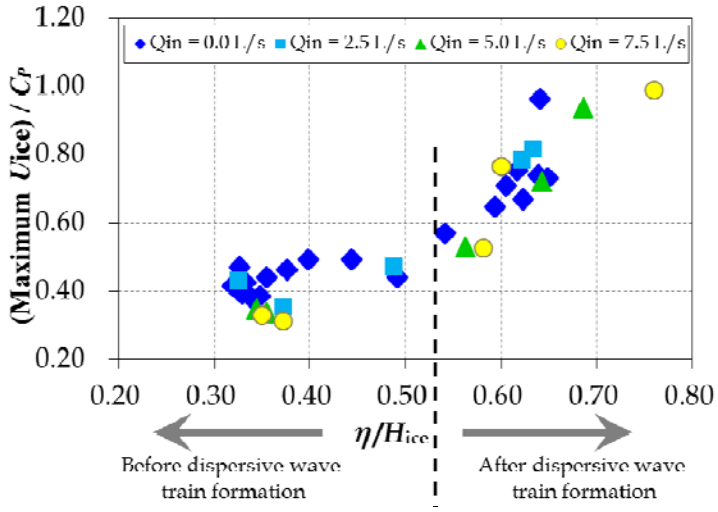

Figure 7. Relationship between wave height-water depth ratio of incident waves and maximum transportation velocity.